Networks and Heterogeneous Media

NHM, 21(6): 2383–2411.
DOI: 10.3934/nhm.2026089
Received: 25 August 2026
Revised: 29 September 2026
Accepted: 12 October 2026
Published: 16 November 2026

https://www.aimspress.com/journal/NHM

Research article

Modeling the impact of adaptive thresholds on information-epidemic co-evolution in multiplex network

Liang'an Huo[1,2,*], Xingyu Wan[1], Xu Xu[1] and Minghua Liu[1]

[1] Business School, University of Shanghai for Science and Technology, Shanghai 200093, China
[2] School of Intelligent Emergency Management, University of Shanghai for Science and Technology, Shanghai 200093, China

* **Correspondence:** Email: huohuolin@yeah.net; Tel: +862165711630.

Abstract: During epidemic outbreaks, individuals often reduce their risk of infection by breaking connections with infected individuals in order to stay in a relatively safe environment. Motivated by these observations, this paper incorporates adaptive thresholds into a multiplex network UA_1A_2U-SIS (unaware–positive–negative–unaware–susceptible–infected–susceptible) model with adaptive mechanisms. In this framework, the effectiveness of adaptive behavior is governed by individual sensitivity threshold functions, enabling the exploration of how adaptive thresholds influence the coupled propagation of information and epidemics. Using the microscopic Markov chain approach (MMCA), we derived the state transition equations and the epidemic transmission threshold. Extensive numerical simulations validate the theoretical analysis and demonstrate that adaptive thresholds play a significant role in shaping both information diffusion and epidemic propagation. Specifically, enhancing individuals' ability to distinguish between positive and negative information, as well as promoting the active adoption of positive information beneficial for epidemic prevention, can effectively suppress epidemic outbreaks. Furthermore, increasing individuals' risk sensitivity promotes more frequent adaptive behaviors, reduces opportunities for infection, and ultimately mitigates the overall epidemic scale.

Keywords: adaptive mechanisms; sensitivity threshold functions; information transmission; epidemic spreading; time-varying multiplex network

1. Introduction

The spread of epidemics has long been a major concern for humanity. In recent years, global epidemics such as SARS, H1N1, and COVID-19 have emerged, posing serious threats to people's lives and property [1–3]. Therefore, it is very important to study the mechanisms of epidemic spreading and propose effective preventive measures. Through extensive research, scientists have proved that wearing masks and maintaining physical distance can effectively restrain epidemic spreading and have provided guidance for controlling epidemics [4–6].

Researchers have a long history of studying epidemic spreading. Among these, the traditional SIR model [7–9] (susceptible–infected–removed) categorizes individuals into three groups and derives thresholds for epidemic spreading. This marks the formal introduction of the currently recognized epidemic spreading dynamics. Researchers subsequently proposed the SIS model [10–12] (susceptible–infected–susceptible). Recently, researchers have integrated SIR and SIS models into complex networks to better capture the impact of interactions among numerous individuals in the real world. This approach successfully demonstrated that epidemic spreading thresholds are influenced by network structure [13–16]. However, in real life, individuals with epidemic-related knowledge can reduce the probability of being infected, suggesting that information may also be a factor influencing epidemic spreading.

Subsequently, researchers introduced information into epidemic spreading models and demonstrated its coupling relationship. Funk et al. [17] investigated the impact of individual information on epidemic spreading dynamics, revealing that information can effectively suppress epidemic spreading. Granell et al. [18] proposed a two-layer $UAU-SIS$ network model coupling information and epidemics. Then, Granell et al. [19] introduced mass media into the information-epidemic multiplex network. Since then, researchers have focused on the coupling of information and epidemics within multiplex networks. Zhang et al. [20] examined indirect information transmission within the information layer. Liu et al. [21] introduced negative information about vaccination. Song et al. [22] investigated the impact of higher-order interactions in the information layer. Yang et al. [23] examined the impact of self-media on information transmission and epidemic spreading. Sun et al. [24] introduced the influence of information verification mechanisms on epidemic spread within multilayer high-order networks. Liu et al. [25] incorporated two distinct cognitive states, positive and negative perceptions of the epidemic, which lead to differing behaviors and infection rates. Results indicate that positive information effectively suppresses epidemic spreading, while negative information can promote epidemic spreading.

Consequently, researchers have begun focusing on adaptive networks. Once a susceptible individual connects to an infected individual, they may break the connection and then seek another susceptible individual to establish a new connection. Guo et al. [26] introduced adaptive networks to deeply examine how adaptive behavior impacts epidemic spreading and network structure. Song et al. [27] studied adaptive networks incorporating spatial distance and connection preference mechanisms. Zhu et al. [28] investigated the impact of exposure on adaptive behavior, where both susceptible individuals and exposed individuals could exhibit adaptive behavior. They concluded that the presence of exposure disrupted the effective implementation of adaptive behavior. Mancastroppa et al. [29] introduced the effects of activity level and attractiveness on adaptive behavior, categorizing adaptive behavior into active quarantine and inactive quarantine. Results indicated that active quarantine more effectively suppresses epidemic spreading. Hong et al. [30] studied how multi-source information affects the

adaptive rewiring mechanism and the dynamics of epidemic spreading. Peng and Zhang [31] introduced the influence of individual information states on adaptive frequency, recognizing that individuals aware of epidemic presence are more inclined to exhibit adaptive behavior. Guo et al. [32] examined the impact of adaptive behavior within the information layer on epidemic dynamics, where individuals aware of the epidemic sever ties with unaware individuals and establish connections with other aware individuals. Xiong and Zhou [33] investigated the impact of higher-order interactions on adaptive networks. Higher-order adaptive behavior may occur, deleting the 2-simplex. Conversely, three susceptible nodes may actively form a 2-simplex. The above studies demonstrate that adaptive behavior significantly influences epidemic spreading, highlighting the substantial practical significance of further research on adaptive networks.

Moreover, the individuals' heterogeneity in real life significantly impacts the scale of epidemic spreading [34–36]. Liu et al. [37] first proposed a complex network model for epidemic spreading incorporating activity. Active nodes proactively interact with all other nodes, while inactive nodes can only passively interact with active nodes. Zhang et al. [38] proposed individuals' heterogeneity in protective behavior tendencies in epidemic spreading. Shi and Zhu [39] introduced an activity-driven network into epidemic spreading, in which active nodes extend links to create new edges with other nodes. Subsequently, Li and Huo [40] introduced threshold functions, in which only if the sum of two nodes' activity exceeds a certain threshold can they build a valid connection. Such previous studies have proved that an individual's heterogeneity has a significant impact on epidemic spreading.

However, prior studies have generally relied on simplified assumptions regarding adaptive behavior, whereby a susceptible node can easily disconnect from an infected node and establish a new connection with another susceptible node. In reality, severing a connection from a certain neighbor is considerably more complex. If a susceptible individual perceives that the infection risk posed by an infected neighbor is relatively low, they may choose not to terminate the connection. Additionally, individuals in real life are willing to receive correct and useful information, but information spread in real life has both correct and incorrect sides. Therefore, individuals may take self-protective behavior to avoid being exposed to incorrect information. Moreover, individuals exhibit heterogeneity in their sensitivity to risk. Those with higher sensitivity can perceive surrounding risks more quickly than those with lower sensitivity and therefore be more inclined to adopt preventive measures. Consequently, highly sensitive individuals are more likely to engage in adaptive behaviors with greater frequency in order to maintain safer environments. Therefore, adaptive behavior in the real world is inherently more complex, and both disconnection and reconnection processes require specific triggering mechanisms. To capture this phenomenon, this paper proposes a new model that more accurately characterizes the impact of individual heterogeneity on adaptive behavior. The main contributions of this paper are summarized as follows:

(1) We assume that adaptive behavior, disconnecting and reconnecting edges, occurs only when the combined sensitivity levels of the two nodes satisfy specific conditions. For disconnection, the sum of the sensitivity levels between the two nodes must exceed a predefined disconnection threshold. Similarly, for reconnection, the sum of their sensitivity levels must exceed a reconnection threshold. Additionally, to distinguish the adaptive reconnection priorities under different infection risks, we introduce an information-reduction factor, whereby different information states influence the reconnection threshold.

(2) We assume that adaptive behavior occurs simultaneously in both the information layer and the epidemic layer. In the information layer, nodes are assumed to behave rationally and exhibit a

preference for positive information. Both positive and negative information coexist within the information layer. Positive information is regarded as correct and useful to epidemic prevention, while negative information is incorrect and harmful to epidemic prevention. Therefore, information adaptive behavior relates to negative information. Unaware nodes actively disconnect from nodes spreading negative information and seek another node that is spreading positive information to establish a new connection.

The remainder of this paper is structured as follows: Section 2 details the sensitivity-driven UA_1A_2U-SIS adaptive model; Section 3 presents the theoretical derivation of our model using the MMCA method; Section 4 demonstrates numerical results via Monte Carlo (MC) simulations; Section 5 summarizes the main conclusions.

2. Model description

In reality, individuals exposed to epidemic spread tend to adopt adaptive behaviors to reduce their risk of infection. They may cut off the edges with infected individuals to minimize the probability of infection and establish a safe edge with other healthy individuals. However, individuals differ in personality and sensitivity levels, which will directly lead to the implementation of adaptive behavior. At the information and epidemic layers, we use sensitivity levels to describe nodes' risk perception sensitivity. Individuals with higher sensitivity are more sensitive to both information transmission and epidemic spreading and can notice risks and react faster than individuals with lower sensitivity. Specifically, individuals with higher sensitivity can identify the risky individuals around them and then apply adaptive behavior in a timely manner; individuals with low sensitivity levels take more time to notice risks and adopt adaptive behavior more slowly. In the information layer, individuals with negative information will adopt incorrect epidemic prevention behavior, and incorrect behavior will increase the infection risk. Therefore, information adaptive behavior will break the negative information transmission channels and seek positive information channels to further lower infection probability. Higher-sensitivity individuals can break the negative channels and find a positive channel faster than individuals with lower sensitivity. Meanwhile, in the epidemic layer, when healthy individuals are connected to infected individuals, higher-sensitivity individuals can break the risky edges and build a healthy edge with another susceptible individual faster than lower-sensitivity individuals.

Thus, this paper proposes a time-varying multiplex network with an adaptive threshold to investigate the impact of adaptive thresholds on the coupled propagation of information and epidemics. The network topology structure will be changed at each time step, indicating the adaptive behavior adopted by individuals. As shown in Figure 1, we introduce the information layer (e.g., WeChat, Weibo, or TikTok) to depict the information transmission process. Simultaneously, we consider the epidemic layer (e.g., schools, dormitories, or companies) to depict the epidemic spreading process. Each node maintains a one-to-one correspondence between the upper and lower layers. We use a normal distribution to describe the heterogeneity of individuals' sensitivity. Heaviside function is used to judge the adaptive behavior. The assumptions of this paper are as follows:

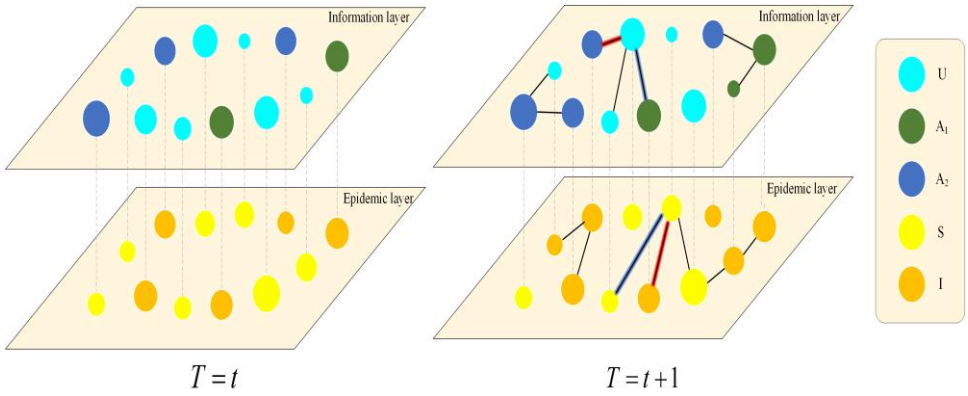


Figure 1. Schematic diagram of a time-varying adaptive network. Different node sizes represent varying sensitivity levels; the larger the node size, the higher the sensitivity level. A red-growing line indicates that the edge that was connected at time t has been disconnected at time $t+1$, while a blue-growing line indicates that an edge that was not connected at time t has been established at time $t+1$.

Assumption 1: The information transmission process

We employ an UA_1A_2U model to describe the information transmission process within the information layer and nodes' opposing perceptions of the epidemic. Nodes in the information layer are categorized into three states: U (unaware), A_2 (positive), and A_2 (negative). Specifically, when a node is in the unaware state, it means that the individual has no idea about the epidemic. A node in the positive state means that the individual has a positive perception of health authorities and will follow official recommendations; therefore, they will take correct and effective measures to protect themselves from being infected. On the contrary, a node in the negative state means that the individual has a negative perception of the health authorities and will not follow official recommendations or will ignore those recommendations, which means the prevention measures they take to protect themselves from being infected are incorrect and useless. An U node can transition to the A_1 or A_2 state with probability λ_1 or λ_2 after receiving positive or negative information from an adjacent A_1 or A_2 node. However, we assume that all nodes are in favor of positive information; U nodes will preferentially transfer to A_2 when receiving both positive and negative information. Also, the U node can transfer to the A_2 state only when the individual did not transfer to A_2. Moreover, we set $\lambda_1 > \lambda_2$ as nodes in favor of positive information. Additionally, both A_1 and A_2 nodes may forget the information with probability δ, reverting to the U state. Figure 2 illustrates the state transitions of information transmission within the information layer.

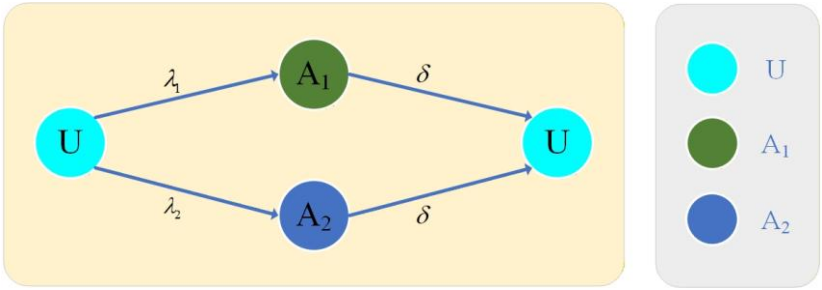


Figure 2. Schematic diagram of information transmission.

Assumption 2: The epidemic spreading process

In the epidemic layer, we employ a SIS model to represent the epidemic spreading process occurring within the epidemic layer. All nodes in the epidemic layer are categorized into S and I states. The S state indicates a node that has not been infected by the epidemic, while the I state indicates a node that has been infected. S nodes can be infected by their adjacent I nodes with probability β, causing them to transition to I nodes with probability β. We hypothesize that a node's differing understandings of the epidemic influence its probability of being infected. We employ β^U, β^{A_1}, and β^{A_2} to denote the distinct infection rates for nodes. Here, $\beta^U = \beta$, $\beta^{A_1} = \gamma_1\beta$, $\beta^{A_2} = \gamma_2\beta$. γ_1 and γ_2 represent reducing and scaling factors for epidemic spreading rates, respectively, where $0 < \gamma_1 < 1 < \gamma_2$. γ_1 ranges from $[0,1]$, meaning that the A_1 nodes can reduce the infection rate due to the correct cognition of epidemic; γ_2 is larger than 1 because A_2 nodes have incorrect cognition of epidemic, which leads to a larger infection rate. Nodes in the A_1 state follow the official recommendations, enabling them to take the most effective measures among the three cognition types. Nodes in A_2 state do not follow the official recommendations, and the measures they take are useless or even harmful. Nodes in the U state are completely unaware of the existence of the epidemic and will not take any measures. Therefore, nodes in the A_1S state have the lowest probability of being infected by adjacent I nodes, followed by nodes in state US, and nodes in the A_2S state have the highest probability of being infected. The probability of the three information state nodes being infected by an adjacent I node is as follows:

$$\beta^X = \begin{cases} \beta & X = U \\ \gamma_1\beta & X = A_1 \\ \gamma_2\beta & X = A_2 \end{cases} \tag{1}$$

where $X \in \{U, A_1, A_2\}$. Additionally, an infected node I has a probability μ of being cured and transitioning to the S state. Figure 3 illustrates the state transition diagram of epidemic spreading occurring within the epidemic layer.

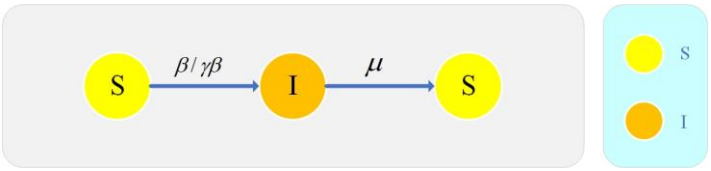


Figure 3. Schematic diagram of epidemic spreading.

Assumption 3: Sensitivity-driven time-varying adaptive network

Based on the original activity-driven network [39], we reinterpret the activity level as a sensitivity level to reflect individual heterogeneity in risk perception and use the same network generation mechanism. Therefore, we employ a sensitivity-driven time-varying adaptive network to represent the network structure that changes over time in both the information and epidemic layers, respectively. In real life, the neighbors of each node often differ across time periods, such as during work hours and after work. Adaptive behavior will change the topology structure of the network. The N nodes in the information layer and epidemic layer are assigned sensitivity levels a and b, respectively. We assume the sensitivity level is a number that follows a normal distribution within the range $[0,1]$. Once assigned, the sensitivity level remains unchanged.

$$F(a_i) = \frac{1}{\sqrt{2\pi}\sigma_1}\exp(-\frac{(a_i - \chi_1)^2}{2\sigma_1}), \tag{2}$$

$$F(b_i) = \frac{1}{\sqrt{2\pi}\sigma_2}\exp(-\frac{(b_i - \chi_2)^2}{2\sigma_2}), \tag{3}$$

here, Eqs (2) and (3) are used as weight functions with an approximately normal shape, rather than strictly normalized probability-density functions on [0,1]. Since the sensitivity levels are restricted to [0,1], the Gaussian expressions are truncated without renormalization, and the values are interpreted as relative weights in the numerical simulations. χ_1, χ_2 denote the average sensitivity levels of nodes in the information layer and epidemic layer, respectively. We employ asymmetric sensitivity levels to represent the differing online and offline personality of the same node. A larger χ_1, χ_2 indicates a higher average sensitivity of nodes within the corresponding layer. σ_1, σ_2 represent the standard deviations of node sensitivity levels in the information layer and epidemic layer, respectively. A larger σ_1, σ_2 means a greater numerical variation in node sensitivity levels within the corresponding layers.

We define that the sensitivity-driven time-varying network follows these steps: First, at initial time $t = 0$, all nodes in the network are unconnected. Subsequently, at time $t = 1$, nodes in the information layer and epidemic layer become sensitive with probabilities a_i and b_i, respectively. Sensitive nodes in each layer then randomly select nodes to form m_a and m_b connections, respectively. Then, unaware nodes in the information layer and susceptible nodes in the epidemic layer take adaptive behavior.

Assumption 4: Adaptive behavior with sensitivity threshold

This paper assumes that nodes are rational and favor positive information; therefore, adaptive behavior occurs in both the information and epidemic layers. In recent years, researchers have investigated adaptive networks in order to better describe the self-protection behavior driven by rational individuals. A complete and traditional adaptive behavior has two steps. Once a S node is adjacent to an I node, driven by self-preservation, the individual would actively disconnect from the I node and find another S node to create a new connection with probability ω. Although an U node relates to the lack of epidemic-related information, it could distinguish the content of positive and negative information by checking the source of information that was shared by A_1 and A_2, reading comments about the information. Once an U node discovers they are now connecting to an A_2 node, they would disconnect from the A_2 node and immediately seek another A_1 node to create a new connection. In summary, the information adaptive behavior is breaking the $U - A_2$ edges and then creating a new $U - A_1$ edge in the information layer, while the epidemic adaptive behavior breaks the $S - I$ edges and then creates a new $S - S$ edge in the epidemic layer. Therefore, the U node could remove a direct connection with the A_2 node and create a connection with A_1, making sure that no opportunity is transmitted to the negative state. Similarly, the S node could directly eliminate an infection opportunity caused by a neighbor I node, due to the epidemic adaptive behavior of cutting off a direct infection pathway. However, in reality, neither information adaptive behavior nor epidemic adaptive behavior is easily implemented. In the information layer, individuals may be less likely to adopt disconnection behavior when they perceive a low risk of being transmitted negative information from their neighbors. In the epidemic layer, individuals may also be less likely to disconnect from infected neighbors when they perceive a low risk of infection.

Therefore, we use node sensitivity to represent node heterogeneity, where higher sensitivity

indicates more sensitivity to risk. Similarly, sensitivity can be understood as tolerance to risk; higher-sensitivity individuals are very sensitive to the time exposed to risk, and lower-sensitivity individuals are relatively not concerned about exposure to risk. We define a Heaviside function to judge whether adaptive behavior occurs; complete adaptive behavior occurs only after both the reconnection and disconnection thresholds are met. When the sum of two nodes' sensitivity exceeds the disconnection threshold, the edge will be cut off, meaning that this edge is too risky to maintain the connection and needs to break as soon as possible. Similarly, if the sum of two unconnected nodes' sensitivity exceeds the reconnection threshold, a new connection will be built, meaning this newly created edge is relatively safe and there is no need to be concerned about risk. An adaptive behavior assumes that both the disconnection and reconnection thresholds are satisfied; if one threshold is not satisfied, the adaptive behavior will not occur.

To better illustrate the operational mechanism of adaptive thresholds, Figure 4 depicts the adaptive process with adaptive thresholds in both the information layer and epidemic layer. Figure 4(a),(b) depicts the adaptive behavior processes happening between nodes i, j, and k in the information layer and epidemic layer. In both layers, the probability of adaptive behavior occurring is ω. Figure 4(a) depicts the information adaptive behavior with connected U node i and A_2 node j that can disconnect only when the sum of node sensitivity exceeds the information disconnection threshold a_D. Unconnected U node i and A_1 node k can create a new edge only when the sum of sensitivity exceeds the reconnection threshold a_R. Figure 4(b) depicts the epidemic adaptive behavior, where connected S node i and I node j can disconnect only when the sum of node sensitivity exceeds the epidemic disconnection threshold b_D. Unconnected S node i and S node k can create a new edge only when the sum of sensitivity exceeds the reconnection threshold b_R. The red-glowing lines in Figure 4 indicate that the adjacent nodes at time step t disconnected at time step $t+1$.The blue-glowing lines represent two unconnected nodes at time step t that will build a new edge at time step $t+1$. We employ the Heaviside step function $H[\alpha]$ to determine whether disconnection or reconnection can occur during adaptive behavior. Specifically, when $\alpha > 0$, $H[\alpha]=1$. This indicates the node can perform adaptive behavior. Otherwise, $\alpha \le 0$, $H[\alpha]=0$, which means two nodes cannot take adaptive behavior. Thus, for information adaptive behavior, $H[a_i + a_j - a_D]$ and $H[a_i + a_j - a_R]$ can be used to describe whether nodes can meet the information adaptive threshold conditions and successfully take adaptive behavior in the information layer. For the epidemic adaptive behavior, $H[b_i + b_j - b_D]$ and $H[b_i + b_j - b_R]$ can be used to describe whether nodes can meet the epidemic adaptive threshold conditions and successfully take adaptive behavior in the epidemic layer. Although adaptive behavior may temporarily block infection pathways to a susceptible node in the epidemic layer, there is still a possibility that its neighbors will be infected in the next time step. Therefore, the greater the possibility of being infected for newly connected neighbors, the higher the infection risk for the node in the next time step.

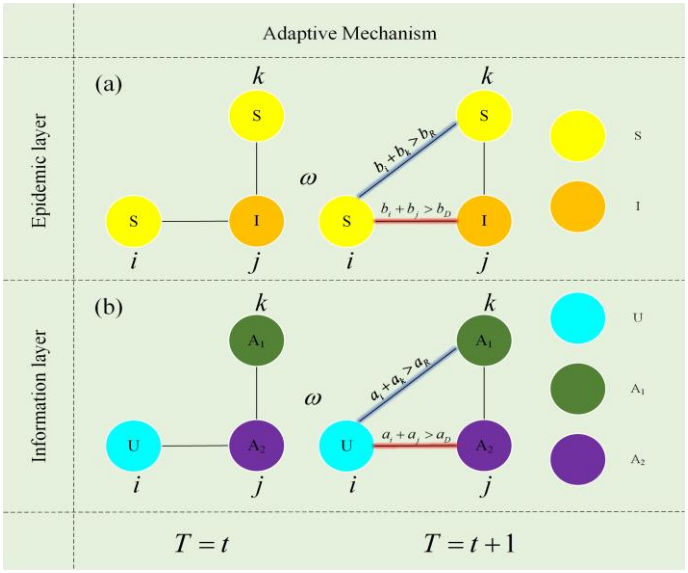


Figure 4. The operational mechanism of adaptive thresholds. (a) and (b) depict the progression of adaptive behavior within the epidemic layer and information layer, respectively. The red-glowing line indicates the disconnection between nodes i and j, followed by the formation of a new blue-glowing link between nodes i and k.

Table 1 shows the definitions of parameters.

Table 1. Definitions of parameters.

Parameter	Definition
λ	The information diffusion rate
β	The epidemic spreading rate
δ	The information forgetting rate
μ	The epidemic recovering rate
a_i	The sensitivity for node i in information layer
b_i	The sensitivity for node i in epidemic layer
φ	Information reduction factor
m_a	The number of links created by the active node in the information layer
m_b	The number of links created by the active node in the epidemic layer
ω	The probability of node adopting adaptive behavior
γ_1	Positive information-reducing factor
γ_2	Negative information scaling factors

Continued on next page

Parameter	Definition
$g_{ijk}^{U}(t)$	Probability that the node i breaks the link with neighbor k and creates a new link with the individual j at time t in the information layer.
$g_{ijk}^{A_1}(t)$	Probability that the A_1S node i breaks the link with neighbor k and creates a new link with the individual j at time t in the epidemic layer.
$g_{ijk}^{A_2}(t)$	Probability that the A_2S node i breaks the link with neighbor k and creates a new link with the individual j at time t in the epidemic layer.
a_R	Adaptive reconnecting threshold in the information layer
a_D	Adaptive disconnecting threshold in the information layer
b_R	Adaptive reconnecting threshold in the epidemic layer
b_D	Adaptive disconnecting threshold in the epidemic layer

Simultaneously, we observe that different viewpoints about epidemics within the information layer directly leads to different infection rates. Therefore, we reasonably employ reducing factors φ, $0<\varphi<1$ to represent the influence of information on reconnection thresholds. Table 2 details the influence of information-reducing factors on epidemic reconnection thresholds. When an A_1S node tries to establish a new connection with a US (A_1S) node, their reconnection threshold stays at b_R. This is because A_2S nodes have a negative perception of the epidemic, leading to higher infection risk, and thus US (A_1S) nodes choose to lower the priority of forming a new connection with A_2S nodes. For two US (A_2S) nodes that have the same perception of the epidemic, their reconnection threshold decreases to φb_R. This indicates that these two nodes have a common interest, choosing to raise the priority of building a new connection. Similarly, when US and A_1S nodes try to form a new connection, their reconnection threshold is φb_R. This is because A_1S nodes' positive perception of the epidemic reduces their infection risk, leading them to increase the priority of connection. For two A_1S nodes, their reconnection threshold will further decrease to $\varphi^2 b_R$. This indicates that, building upon common interest, a positive understanding of the epidemic minimizes the infection risk, thereby having the highest priority of connection.

Table 2. Different epidemic reconnection thresholds.

Threshold	US	A_1S	A_2S
US	φb_R	φb_R	b_R
A_1S	φb_R	$\varphi^2 b_R$	b_R
A_2S	b_R	b_R	φb_R

3. Theoretical analysis

Motivated by previous studies on MMCA to analyze the dynamics of epidemic spreading [41–43],

we use the microscopic Markov chain approach to analyze the dynamics of information and epidemic spreading to obtain accurate theoretical results. Based on the assumptions outlined above, the network may exhibit six possible states: US, UI, A_1S, A_1I, A_2S, and A_2I. We assume that at each time step t, the probabilities of node i being in these six states are, respectively, $P_i^{US}(t)$, $P_i^{UI}(t)$, $P_i^{A_1S}(t)$, $P_i^{A_1I}(t)$, $P_i^{A_2S}(t)$, and $P_i^{A_2I}(t)$, and satisfy $P_i^{US}(t)+P_i^{UI}(t)+P_i^{A_1S}(t)+P_i^{A_1I}(t)+P_i^{A_2S}(t)+P_i^{A_2I}(t)=1$. Let $\phi_i^{A_1}(t)$ denote the probability that node i is not informed with positive information by any A_1 neighbor node at time t, and $\phi_i^{A_2}(t)$ denote the probability that node i is not informed with negative information by any A_2 neighbor node at time t. We can obtain $\phi_i^{A_1}(t)$, $\phi_i^{A_2}(t)$:

$$\phi_i^{A_1}(t)=\prod_j[1-\lambda_1 d_{ij}^1(t)\frac{m_a}{N}[a_i P_j^{A_1}(t)+a_j P_j^{A_1}(t)]] \tag{4}$$

$$\phi_i^{A_2}(t)=\prod_j[1-\lambda_2 d_{ij}^1(t)\frac{m_a}{N}[a_i P_j^{A_2}(t)+a_j P_j^{A_2}(t)]] \tag{5}$$

where $P_i^{A_1}(t)=P_i^{A_1S}(t)+P_i^{A_1I}(t)$, $P_i^{A_2}(t)=P_i^{A_2S}(t)+P_i^{A_2I}(t)$. Also, $d_{ij}^1(t)\frac{m_a}{N}[a_i P_j^{A_1}(t)+a_j P_j^{A_1}(t)]$ denotes the probability that node j is a neighbor of node i at time t, while m_a represents the number of edges extended by a node in the information layer after activation. Specifically, $\frac{m_a}{N}a_i P_j^{A_1}(t)$ indicates that after node i is activated, it extends an edge to node j in state A_1, becoming an adjacent node. Similarly, $\frac{m_a}{N}a_j P_j^{A_1}(t)$ denotes that after node j in state A_1 is activated, it extends an edge to node i, becoming an adjacent node.

Due to the existence of adaptive behavior, node i and j may be disconnected from each other. Therefore, we need to make sure they have a certain edge after adopting adaptive behavior [32]. Among these, $d_{ij}^1(t)$ denotes whether nodes i and j in the information layer are connected at time t. If $d_{ij}^1(t)=1$, then they are connected. If $d_{ij}^1(t)=0$, then they are not connected.

We use $r_i^{A_1}(t)$ and $r_i^{A_2}(t)$ to denote the probability that a node i in state U is transformed into states A_1 and A_2 by its adjacent nodes at time t, respectively. We also use $r_i^U(t)$ to denote the probability that node i in state U is not informed by its adjacent nodes at time t.

$$r_i^U(t)=\phi_i^{A_1}(t)\phi_i^{A_2}(t), \tag{6}$$

$$r_i^{A_1}(t)=1-\phi_i^{A_1}(t), \tag{7}$$

$$r_i^{A_2}(t)=\phi_i^{A_1}(t)[1-\phi_i^{A_2}(t)]. \tag{8}$$

Let $q_i^U(t)$, $q_i^{A_1}(t)$, and $q_i^{A_2}(t)$ denote the probabilities that US, A_1S, and A_2S state nodes i are not infected by the neighboring infected nodes at time t. We obtain:

$$q_i^U(t)=\prod_j[1-\beta^U d_{ij}^2(t)\frac{m_b}{N}[b_i P_j^I(t)+b_j P_j^I(t)]] \tag{9}$$

$$q_i^{A_1}(t)=\prod_j[1-\beta^{A_1} d_{ij}^2(t)\frac{m_b}{N}[b_i P_j^I(t)+b_j P_j^I(t)]] \tag{10}$$

$$q_i^{A_2}(t)=\prod_j[1-\beta^{A_2} d_{ij}^2(t)\frac{m_b}{N}[b_i P_j^I(t)+b_j P_j^I(t)]] \tag{11}$$

Among these, $P_i^S(t)=P_i^{US}(t)+P_i^{A_1S}(t)+P_i^{A_2S}(t)$, $P_i^I(t)=P_i^{UI}(t)+P_i^{A_1I}(t)+P_i^{A_2I}(t)$. Similarly, $d_{ij}^2(t)$ denotes whether nodes i and j are connected in the epidemic layer. We also use $d_{ij}^2(t)$ to ensure nodes i and j are still connected in the epidemic layer after the nodes adopt epidemic adaptive behavior at time t. If $d_{ij}^2(t)=1$, then they are connected. If $d_{ij}^2(t)=0$, then they are not connected.

Simultaneously, in the information layer, we use $g_{ijk}^U(t)$ to represent the probability that node i in state US at time t disconnects from node j in state A_2 and creates a new connection with node k in state A_1. We can derive that:

$$\begin{aligned} g_{ijk}^U(t)=\omega P_i^U(t)&\frac{P_j^{A_2}(t)H[a_i+a_j-a_D]}{\sum_{h=1,h\neq j}^{n} d_{jh}^1(t)P_h^{A_2}(t)+P_j^{A_2}(t)}\\ &\cdot\frac{P_j^{A_1}(t)H[a_i+a_k-a_R]}{\sum_{h=1,h\neq k}^{n}(1-d_{jh}^1(t))P_h^{A_1}(t)+P_k^{A_1}(t)},i\neq j=1,2,\cdots,n \end{aligned} \tag{12}$$

$g_{ijk}^{A_1}(t)$ and $g_{ijk}^{A_2}(t)$ denote the probability that a node i in state A_1S and A_2S, respectively, at time t in the epidemic layer, after disconnecting from a node j in state I, establishes a new connection with another node k in state S. We can derive:

$$\begin{aligned} g_{ijk}^{A_1}(t)=\omega P_i^{A_1S}(t)&\frac{P_j^I(t)H[b_i+b_j-b_D]}{\sum_{h=1,h\neq j}^{n} d_{jh}^2(t)P_h^I(t)+P_j^I(t)}\\ &\cdot\frac{P_j^S(t)H[b_i+b_k-b_R]}{\sum_{h=1,h\neq k}^{n}(1-d_{jh}^2(t))P_h^I(t)+P_k^S(t)},i\neq j=1,2,\cdots,n \end{aligned} \tag{13}$$

$$\begin{aligned} g_{ijk}^{A_2}(t)=\omega P_i^{A_2S}(t)&\frac{P_j^I(t)H[b_i+b_j-b_D]}{\sum_{h=1,h\neq j}^{n} d_{jh}^2(t)P_h^I(t)+P_j^I(t)}\\ &\cdot\frac{P_j^S(t)H[b_i+b_k-b_R]}{\sum_{h=1,h\neq k}^{n}(1-d_{jh}^2(t))P_h^I(t)+P_k^S(t)},i\neq j=1,2,\cdots,n \end{aligned} \tag{14}$$

Using Eqs (12)–(14), we can derive the probability evolution equations for nodes i and j connected in the information layer and epidemic layer, respectively:

$$\begin{aligned} d_{ij}^{1}(t+1) = {} & d_{ij}^{1}(t)[1-\omega P_i^{U}(t)\frac{P_j^{A_2}(t)H[a_i+a_j-a_D]}{\sum_{h=1,h\neq j}^{n} d_{jh}^{1}(t)P_h^{A_2}(t)+P_j^{A_2}(t)} \\ & -\omega P_i^{A_2}(t)\frac{P_j^{U}(t)H[a_i+a_j-a_D]}{\sum_{h=1,h\neq j}^{n} d_{jh}^{1}(t)P_h^{A_2}(t)+P_j^{U}(t)}] \\ & +[1-d_{ij}^{1}(t)][1-[1-\omega P_i^{U}(t)\frac{P_j^{A_1}(t)H[a_i+a_k-a_R]}{\sum_{h=1,h\neq j}^{n}(1-d_{jh}^{1}(t))P_h^{A_1}(t)+P_j^{A_1}(t)} \\ & \cdot[1-\omega P_i^{A_1}(t)\frac{P_j^{U}(t)H[a_i+a_k-a_R]}{\sum_{h=1,h\neq j}^{n}(1-d_{jh}^{1}(t))P_h^{U}(t)+P_j^{U}(t)}]] \end{aligned} \tag{15}$$

The first part of Eq (15) represents the probability that connected nodes i and j at time t remain connected at the next time step $t+1$. The second part represents the probability that disconnected nodes i at time t become connected at the next time step $t+1$.

$$\begin{aligned} d_{ij}^{2}(t+1) = {} & d_{ij}^{2}(t)[1-\omega P_i^{S}(t)\frac{P_j^{I}(t)H[b_i+b_j-b_D]}{\sum_{h=1,h\neq j}^{n} d_{jh}^{2}(t)P_h^{I}(t)+P_j^{I}(t)} \\ & -\omega P_i^{I}(t)\frac{P_j^{S}(t)H[b_i+b_j-b_D]}{\sum_{h=1,h\neq j}^{n} d_{jh}^{2}(t)P_h^{S}(t)+P_j^{S}(t)}] \\ & +[1-d_{ij}^{2}(t)][1-[1-\omega P_i^{S}(t)\frac{P_j^{S}(t)H[b_i+b_k-b_R]}{\sum_{h=1,h\neq j}^{n}[1-d_{jh}^{2}(t)]P_h^{S}(t)+P_j^{S}(t)} \\ & \cdot[1-\omega P_i^{S}(t)\frac{P_j^{S}(t)H[b_i+b_k-b_R]}{\sum_{h=1,h\neq j}^{n}[1-d_{jh}^{2}(t)]P_h^{S}(t)+P_j^{S}(t)}]] \end{aligned} \tag{16}$$

$$\begin{aligned} d_{ij}^{SI}(t+1) = d_{ij}^{SI}(t)d_{ij}^{2}(t+1) = {} & d_{ij}^{2}(t)[1-\omega P_i^{S}(t)\frac{P_j^{I}(t)H[b_i+b_j-b_D]}{\sum_{h=1,h\neq j}^{n} d_{jh}^{2}(t)P_h^{I}(t)+P_j^{I}(t)} \\ & -\omega P_i^{I}(t)\frac{P_j^{S}(t)H[b_i+b_j-b_D]}{\sum_{h=1,h\neq j}^{n} d_{jh}^{2}(t)P_h^{S}(t)+P_j^{S}(t)}] \end{aligned} \tag{17}$$

where d_{ij}^{SI} is the $S-I$ edge connection matrix; if $d_{ij}^{SI}=1$, there is an $S-I$ edge connected between node i and j.

Based on Eqs (6)–(11) and the probability transition tree diagram in Figure 5, the MMCA state transition equations for node i in the UA_1A_2U-SIS model can be derived as follows:

$$\begin{aligned} P_i^{US}(t+1) &= P_i^{US}(t)r_i^U(t)q_i^U(t) + P_i^{A_1S}(t)q_i^{A_1}(t)\delta + P_i^{A_2S}(t)q_i^{A_2}(t)\delta + P_i^{UI}(t)r_i^U(t)\mu \\ &\quad + [P_i^{A_1I}(t) + P_i^{A_2I}(t)]\mu\delta \end{aligned} \tag{18}$$

$$\begin{aligned} P_i^{UI}(t+1) &= P_i^{US}(t)r_i^U(t)[1-q_i^U(t)] + P_i^{UI}(t)r_i^U(t)(1-\mu) \\ &\quad + P_i^{A_1S}(t)[1-q_i^{A_1}(t)]\delta + P_i^{A_2S}(t)][1-q_i^{A_2}(t)]\delta + [P_i^{A_1I}(t) + P_i^{A_2I}(t)]\delta(1-\mu) \end{aligned} \tag{19}$$

$$\begin{aligned} P_i^{A_1S}(t+1) &= P_i^{US}(t)q_i^{A_1}(t)r_i^{A_1}(t) + P_i^{UI}(t)\mu r_i^{A_1}(t) + P_i^{A_1S}(t)(1-\delta)q_i^{A_1}(t) \\ &\quad + P_i^{A_1I}(t)(1-\delta)\mu \end{aligned} \tag{20}$$

$$\begin{aligned} P_i^{A_2S}(t+1) &= P_i^{US}(t)q_i^{A_2}(t)r_i^{A_2}(t) + P_i^{UI}(t)\mu r_i^{A_2}(t) + P_i^{A_2S}(t)(1-\delta)q_i^{A_2}(t) \\ &\quad + P_i^{A_2I}(t)(1-\delta)\mu \end{aligned} \tag{21}$$

$$\begin{aligned} P_i^{A_1I}(t+1) &= P_i^{US}(t)[1-q_i^U(t)]r_i^{A_1}(t) + P_i^{UI}(t)(1-\mu)r_i^{A_1}(t) \\ &\quad + P_i^{A_1S}(t)(1-\delta)[1-q_i^{A_1}(t)] + P_i^{A_1I}(t)(1-\delta)(1-\mu) \end{aligned} \tag{22}$$

$$\begin{aligned} P_i^{A_2I}(t+1) &= P_i^{US}(t)[1-q_i^U(t)]r_i^{A_2}(t) + P_i^{UI}(t)(1-\mu)r_i^{A_2}(t) \\ &\quad + P_i^{A_2S}(t)[1-q_i^{A_2}(t)](1-\delta) + P_i^{A_2I}(t)(1-\delta)(1-\mu) \end{aligned} \tag{23}$$

We can let $t\to\infty$, in which the network is in a stable state [44,45], meaning that the state of all nodes in the network will no longer change, which means $P_i(t+1)=P_i(t)$. Simultaneously, we must calculate the threshold β_c at which epidemic spreading begins. When the epidemic spreading rate approaches this threshold, the number of nodes in the UI, A_1I, and A_2I states approaches zero, which means $P_i^{UI}\ll 1$, $P_i^{A_1I}\ll 1$, and $P_i^{A_2I}\ll 1$. Substituting these into Eq (9) yields the following approximate relationship:

$$\begin{aligned} q_i^U(t) &= \prod_j (1-\beta^U d_{ij}^2(t)\frac{m_b}{N}[b_i P_j^I(t) + b_j P_j^I(t)]) \\ &\approx 1-\sum_J \beta^U d_{ij}^2(t)\frac{m_b}{N}[b_i P_j^I(t) + b_j P_j^I(t)] \\ &= 1-\beta^U d_{ij}^2 m_b[b_i \rho^I + \theta_b^I] \\ &= 1-\beta d_{ij}^2 m_b[b_i \rho^I + \theta_b^I] \end{aligned} \tag{24}$$

Similarly, approximating from Eqs (10) and (11), we obtain:

$$\begin{aligned} q_i^{A_1}(t) &= \prod_j (1-\beta^{A_1} d_{ij}^2(t)\frac{m_b}{N}[b_i P_j^I(t)+b_j P_j^I(t)]) \\ &\approx 1-\sum_J \beta^{A_1} d_{ij}^2(t)\frac{m_b}{N}[b_i P_j^I(t)+b_j P_j^I(t)] \\ &=1-\beta^{A_1} d_{ij}^2 m_b[b_i \rho^I+\theta_b^I] \\ &=1-\gamma_1\beta d_{ij}^2 m_b[b_i \rho^I+\theta_b^I] \end{aligned} \tag{25}$$

$$\begin{aligned} q_i^{A_2}(t) &= \prod_j (1-\beta^{A_2} d_{ij}^2(t)\frac{m_b}{N}[b_i P_j^I(t)+b_j P_j^I(t)]) \\ &\approx 1-\sum_J \beta^{A_2} d_{ij}^2(t)\frac{m_b}{N}[b_i P_j^I(t)+b_j P_j^I(t)] \\ &=1-\beta^{A_2} d_{ij}^2 m_b[b_i \rho^I+\theta_b^I] \\ &=1-\gamma_2 d_{ij}^2\beta m_b[b_i \rho^I+\theta_b^I] \end{aligned} \tag{26}$$

where

$$\rho^I=\frac{1}{N}\sum_{j=1}^N P_j^I,\ \theta_b^I=\frac{1}{N}\sum_{j=1}^N b_j P_j^I.$$

Substituting Eq (11) into Eq (7), we obtain the state equation for the system in steady state:

$$\begin{aligned} P_i^{US} &= P_i^{US} r_i^U[1-\beta d_{ij}^2 m_b(b_i\rho^I+\theta_b^I)]+P_i^{A_1S}[1-\gamma_1\beta d_{ij}^2 m_b(b_i\rho^I+\theta_b^I)]\delta \\ &\quad + P_i^{A_2S}[1-\gamma_2\beta d_{ij}^2 m_b(b_i\rho^I+\theta_b^I)]\delta+(P_i^{A_1I}+P_i^{A_2I})\delta\mu \end{aligned} \tag{27}$$

$$\begin{aligned} P_i^{A_1S} &= P_i^{US} r_i^U[1-\gamma_1\beta d_{ij}^2 m_b(b_i\rho^I+\theta_b^I)]+P_i^{UI}\mu r_i^{A_1}+P_i^{A_1S}\delta[1-\gamma_1\beta d_{ij}^2 m_b(b_i\rho^I+\theta_b^I)] \\ &\quad + P_i^{A_1I}(1-\delta)\mu \end{aligned} \tag{28}$$

$$\begin{aligned} P_i^{A_2S} &= P_i^{US}[1-\gamma_2\beta d_{ij}^2 m_b(b_i\rho^I+\theta_b^I)]r_i^{A_2}+P_i^{UI}\mu[(1-r_i^{A_1}) \\ &\quad + P_i^{A_2S}(1-\delta)[1-\gamma_2\beta d_{ij}^2 m_b(b_i\rho^I+\theta_b^I)] \\ &\quad + P_i^{A_2I}(1-\delta)\mu \end{aligned} \tag{29}$$

$$\begin{aligned} P_i^{UI} &= P_i^{US} r_i^U\beta d_{ij}^2 m_b(b_i\rho^I+\theta_b^I)+P_i^{UI} r_i^U(1-\mu)+P_i^{A_1S}\delta\gamma_1\beta d_{ij}^2 m_b(b_i\rho^I+\theta_b^I) \\ &\quad + P_i^{A_2S}\delta\gamma_2\beta d_{ij}^2 m_b(b_i\rho^I+\theta_b^I)+(P_i^{A_1I}+P_i^{A_2I})\delta(1-\mu) \end{aligned} \tag{30}$$

$$\begin{aligned} P_i^{A_1I} &= P_i^{US}\beta d_{ij}^2 m_b(b_i\rho^I+\theta_b^I)r_i^{A_1}+P_i^{UI}(1-\mu)r_i^{A_1}+P_i^{A_1S}(1-\delta)\gamma_1\beta d_{ij}^2 m_b(b_i\rho^I+\theta_b^I) \\ &\quad + (1-\delta)(1-\mu)P_i^{A_1I} \end{aligned} \tag{31}$$

$$
\begin{aligned}
P_i^{A_2 I} = {} & P_i^{US}\beta d_{ij}^2 m_b (b_i \rho^I + \theta_b^I) r_i^{A_2} + P_i^{UI}(1-\mu)(1-r_i^{A_1}) \\
& + P_i^{A_2 S}(1-\delta)\gamma_2 \beta d_{ij}^2 m_b (b_i \rho^I + \theta_b^I) \\
& + (1-\delta)(1-\mu) P_i^{A_2 I}
\end{aligned} \tag{32}
$$

$$
P_i^I = P_i^I (1-\mu) + [P_i^{US}\beta + P_i^{A_2 I}\gamma_1 \beta + P_i^{A_2 S}\gamma_2 \beta](1-\delta) d_{ij}^2 m_b (b_i \rho^I + \theta_b^I) \tag{33}
$$

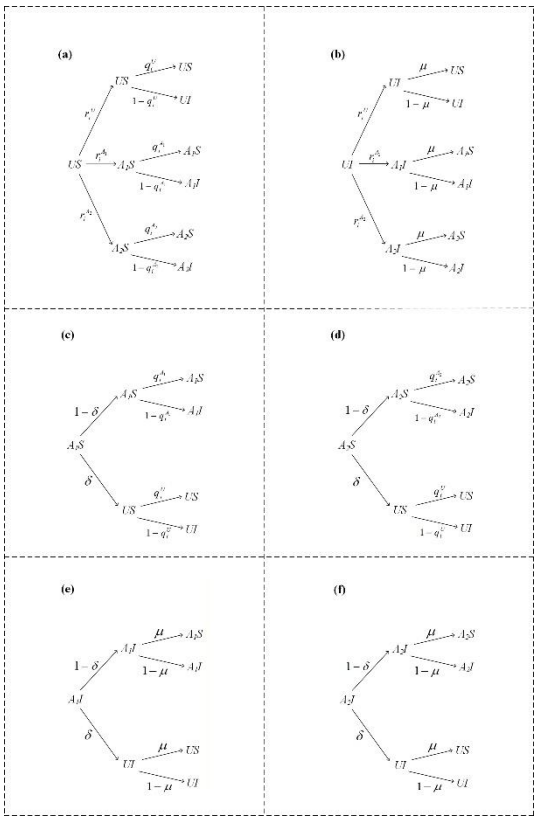


Figure 5. Probability tree of state transfers for node i.

Since the network has reached steady state, $P_i^I \to 0$, we set $P_i^I = P_i^{A_1 I} + P_i^{A_2 I} + P_i^{UI} = \varepsilon_i \ll 1$. Simultaneously, $P_i^U = P_i^{US} + P_i^{UI} \approx P_i^{US}$, $P_i^{A_1} = P_i^{A_1 S} + P_i^{A_1 I} \approx P_i^{A_1 S}$, $P_i^{A_2} = P_i^{A_2 S} + P_i^{A_2 I} \approx P_i^{A_2 S}$. Omitting all first-order $O(\varepsilon)$ and second-order $O(\varepsilon^2)$, we can derive, from Eqs (26)–(31),

$$
P_i^U = P_i^U r_i^U + (P_i^{A_1} + P_i^{A_2})\delta, \tag{34}
$$

$$
P_i^{A_1} = P_i^U r_i^{A_1} + P_i^{A_1}(1-\delta), \tag{35}
$$

$$
P_i^{A_2} = P_i^U r_i^{A_2} + P_i^{A_2}(1-\delta), \tag{36}
$$

$$\begin{aligned} P_i^I &= P_i^I(1-\mu) + P_i^{US}\beta d_{ij}^2 m_b(b_i\rho^I(t)+\theta_b^I) + P_i^{A_1S}\gamma_1\beta d_{ij}^2 m_b(b_i\rho^I(t)+\theta_b^I) \\ &\quad + P_i^{A_2S}\gamma_2\beta d_{ij}^2 m_b(b_i\rho^I(t)+\theta_b^I) \\ &= \varepsilon_i(1-\mu) + (P_i^{US} + P_i^{A_1}\gamma_1 + P_i^{A_2}\gamma_2)\beta d_{ij}^2 m_b(b_i\rho^I(t)+\theta_b^I) \end{aligned} \tag{37}$$

Under the normalization condition $P_i^U + P_i^{A_1} + P_i^{A_2} = 1$, we can further simplify Eq (36) to obtain

$$\varepsilon\mu = [1-(1-\gamma_1)P_i^{A_1S} - (1-\gamma_2)P_i^{A_2S}]\beta d_{ij}^2 m_b(b_i\rho^I(t)+\theta_b^I) \tag{38}$$

by simultaneously dividing Eq (14) by N and then multiplying it by the node epidemic layer sensitivity level b_i. Moreover, we introduce the average connected degree $\overline{d^{SI}}$ [41], where

$$\overline{d^{SI}} = \frac{1}{N}\sum_{i,j} d_{ij}^2 P_i^S P_j^I .$$

The average connected degree $\overline{d^{SI}}$ represents the validated connected $S-I$ edges in the network; therefore, we can use $\overline{d^{SI}}$ to indirectly represent the frequency of adaptive behavior adopted by nodes. The smaller the $\overline{d^{SI}}$, the more frequently adaptive behavior is adopted by nodes.

We obtain

$$\varepsilon\mu = \beta\overline{d^{SI}} m_b(\rho^I(t)Z_b^A + \theta_b^I T^A), \tag{39}$$

$$\theta_b^I\mu = \beta\overline{d^{SI}} m_b(\rho^I(t)Z_{b^2}^A + \theta_b^I Z_b^A), \tag{40}$$

where

$$T^I = \frac{1}{N}\sum_{j=1}([1-(1-\gamma_1)P_j^{A_1} - (1-\gamma_2)P_j^{A_2}]$$

$$Z_b^I = \frac{1}{N}\sum_{j=1} b_j([1-(1-\gamma_1)P_j^{A_1S} - (1-\gamma_2)P_j^{A_2S}]$$

$$Z_{b^2}^I = \frac{1}{N}\sum_{j=1} b_j^2\ ([1-(1-\gamma_1)P_j^{A_1S} - (1-\gamma_2)P_j^{A_2S}]$$

We can rewrite Eqs (15) and (16) in the form of matrix multiplication:

$$\overline{d^{SI}} L\begin{bmatrix}\rho^I \\ \theta_b^I\end{bmatrix} = \frac{\mu}{\beta m_b}\begin{bmatrix}\rho^I \\ \theta_b^I\end{bmatrix}$$

where

$$L = \begin{bmatrix} Z_b^I & T^I \\ Z_{b^2}^I & Z_b^I \end{bmatrix}$$

We use β_c to denote the threshold at which epidemic spreading begins. When $\beta > \beta_c$, the

epidemic starts spreading through the network and eventually reaches a steady state. When $\beta \le \beta_c$, the epidemic cannot propagate within the network. β_c is the minimum value satisfying Eq (16), and $\Lambda_{\max}(L) = \sqrt{Z^I_{b^2} T^I} + Z^I_b$ is the maximum eigenvalue of L.

$$\Lambda_{\max}(L) = \sqrt{Z^I_{b^2} T^I} + Z^I_b .$$

Therefore, we can obtain the threshold for epidemic spreading as

$$\beta_c = \frac{\mu}{\overline{d^{SI}} m_b \Lambda_{\max}(L)}$$

4. Numerical result

In this section, we employ extensive Monte Carlo simulations to prove the accuracy of the adaptive network model and results derived from MMCA. Both layers are generated by sensitivity-driven time-varying networks, with each layer containing nodes $N = 1000$. In both the information layer and epidemic layer, each activated node extends $m_a = 4$, $m_b = 2$ edges to other nodes. The sensitivity of nodes in both layers follows normal distributions with parameters $\chi_1 = \chi_2 = 0.5$ and $\sigma_1 = \sigma_2 = 0.3$. The relationship between the average degree $\langle k_a \rangle$ of the information layer and the average degree $\langle k_b \rangle$ of the epidemic layer is $\langle k_a \rangle = 2\langle k_b \rangle$. Each MC simulation runs for 50 time steps to reduce randomness. At the network's initial state, 10% of nodes in the information layer are set to positive and negative states, while 10% of nodes in the epidemic layer are set to infected states $P^I_i = P^{A_1}_i = P^{A_2}_i = 0.1$. Infected nodes have a probability of $\mu = 0.3$ of recovering to a susceptible state. We set positive and negative information transmission $\lambda_1 = \lambda_2 = \lambda$; meanwhile, positive and negative nodes each have a probability of $\delta = 0.3$ of forgetting information and reverting to an unaware state. Let the information-reducing factor be $\varphi = 0.8$. We set the positive and negative reducing and scaling factors $\gamma_1 = 0.5$ and $\gamma_2 = 1.2$, respectively. We explore the effects of adaptive disconnection and reconnection thresholds in node information states on the final scale of epidemic spread.

4.1. Comparison between Monte Carlo and microscopic Markov chain approach

We investigate the validation of theoretical predictions of the final scale of epidemic spreading dynamics and spreading threshold by comparing Monte Carlo simulations on the specific network topology under different adaptive behavior probability ω. As shown in Figure 6, we can observe that the two methods have strong agreement. The adaptive behavior probability ω has a negative correlation with spreading dynamic ρ^I, and delays the spreading threshold β_c; the final scale of epidemic spreading ρ^I can be controlled as the value of adaptive behavior probability ω increases. This implies that the adaptive behavior can effectively control the spreading dynamics of the epidemic. However, we can also observe that, once the infection rate β exceeds the epidemic threshold β_c, the rate of increase in the scale of the epidemic ρ^I is relatively fast; this implies that the impact of adaptive behavior on the epidemic may delay the epidemic outbreak and restrain the scale of the epidemic; the impact on the rate of epidemic spreading is relatively small.

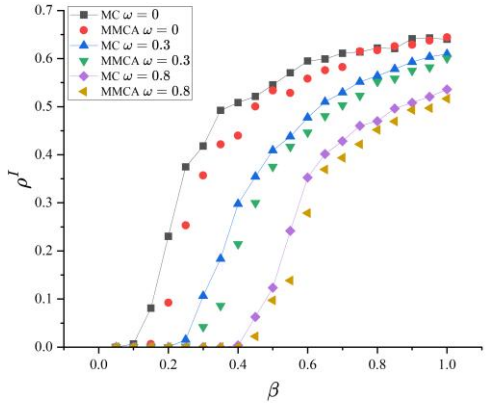


Figure 6. The MC simulation result and MMCA result. Both methods are shown as the final scale of epidemic ρ^I as a function of infection rate β under different adaptive behavior probability ω. Other paraments are set as $a_D = a_R = b_D = b_R = 0.5$, $\lambda = 0.5$, $\varphi = 0.8$.

4.2. Impact of epidemic adaptive thresholds on epidemic spreading

In this section, we primarily investigate the impact of epidemic adaptive thresholds on epidemic spreading. We examine the effects of the disconnection threshold b_D and reconnection threshold b_R on epidemic spreading dynamics. Figure 7(a)–(c) illustrates ρ^I as a function of epidemic spreading probability β and information transmission probability λ under different disconnection threshold b_D and reconnection threshold b_R. A smaller disconnection threshold b_D effectively suppresses the final scale of epidemic spreading and increases the epidemic spreading threshold as well. This occurs because breaking an edge requires the sum of sensitivities to be greater than the disconnection threshold b_D. When it is smaller, there are more nodes that satisfy the threshold, increasing the frequency of adaptive behavior in the network. S nodes continuously stay in a safer environment. Correspondingly, Figure 7(d)–(f) reveals that the impact of the reconnection threshold b_R on epidemic spreading is similar to that of the disconnection threshold b_R. Results show that a larger reconnection threshold b_R leads to a larger scale of epidemic spreading and a smaller spreading threshold. This occurs because establishing new edges requires the sum of node sensitivity to exceed the reconnection threshold b_R. When it is larger, it becomes more difficult for the sum of node sensitivity to surpass b_R, thereby reducing the frequency of adaptive behavior in the network. More $S-I$ edges remain in the network, and S nodes are still connected to their I neighbors, leading to an easier epidemic spreading. To further investigate the impact of epidemic disconnection thresholds b_D and reconnection thresholds b_R on the final epidemic scale, Figure 8 depicts the functional relationship of the final scale ρ^I, disconnection thresholds b_D, and reconnection thresholds b_R.

As shown in Figure 8(a),(b), we observe that both the reconnection threshold b_R and disconnection threshold b_D have a small influence on epidemic spreading when they are set to small values. This occurs because when b_R and b_D are small, nearly all nodes in the network satisfy the adaptive threshold condition. Consequently, the epidemic adaptive threshold has a negative correlation with the epidemic threshold β_c and the scale of epidemic spreading ρ^I, and adjusting the adaptive threshold within a certain range does not affect the frequency of adaptive processes within the network. However, as b_R and b_D increase to a certain threshold, more nodes become unable to satisfy the

adaptive threshold, meaning more S nodes stay with I nodes, therefore promoting epidemic spreading. This manifests as an increase in epidemic spreading scale and a decrease in the spreading threshold, as b_R and b_D increase. Therefore, in real life, maintaining a safe distance from infected nodes, or even actively seeking disconnection to completely break contact, can effectively reduce our probability of infection and limit the scale of epidemic spread.

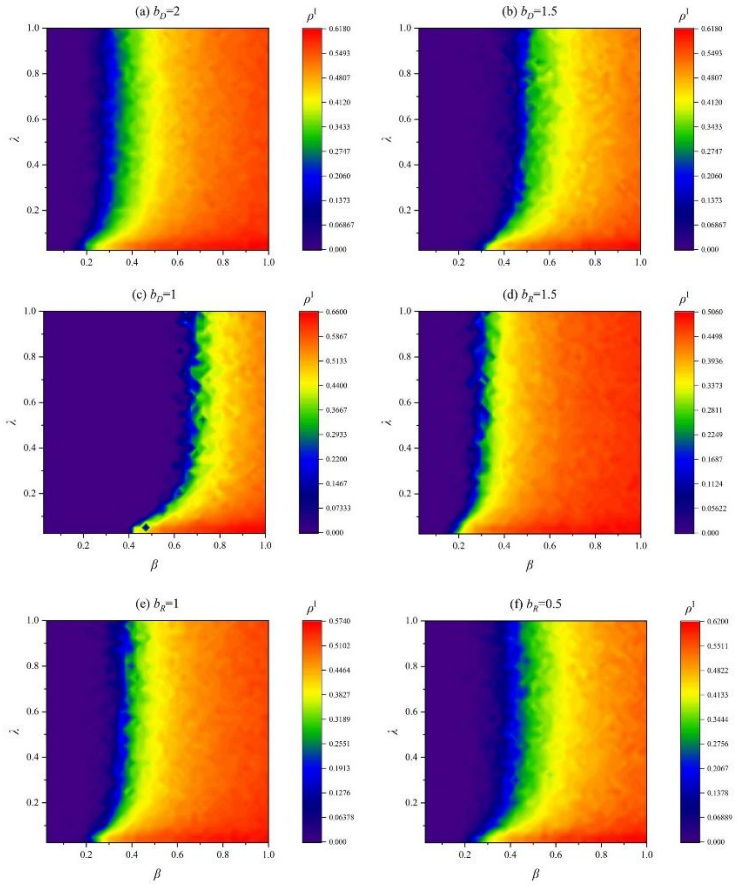


Figure 7. Functional relationship of the infection probability β, information transmission probability λ, and final epidemic scale ρ^I under different epidemic adaptive reconnection thresholds b_R. All MC simulations were conducted with 50 independent iterations. The reconnection thresholds were set to (a) $b_D = 2$, (b) $b_D = 1.5$, and (c) $b_D = 1$. Other parameters were $\omega = 0.8$, $a_D = 1.3$, $a_R = b_R = 1$. The disconnection thresholds were set to (d) $b_R = 1.5$, (e) $b_R = 1$, and (f) $b_R = 0.5$. Other parameters were $\omega = 0.8$, $a_R = 1$, and $a_D = b_D = 0.7$.

From an epidemic prevention perspective, to effectively restrain epidemic spreading, governments and media should actively guide individuals to distinguish infected from healthy individuals, promptly implement adaptive behavior, and avoid contact with infected persons. Simultaneously, cost must be considered: when the majority of individuals can accurately identify infected individuals and promptly adopt adaptive behavior, publicity can be reduced to minimize unnecessary expenses.

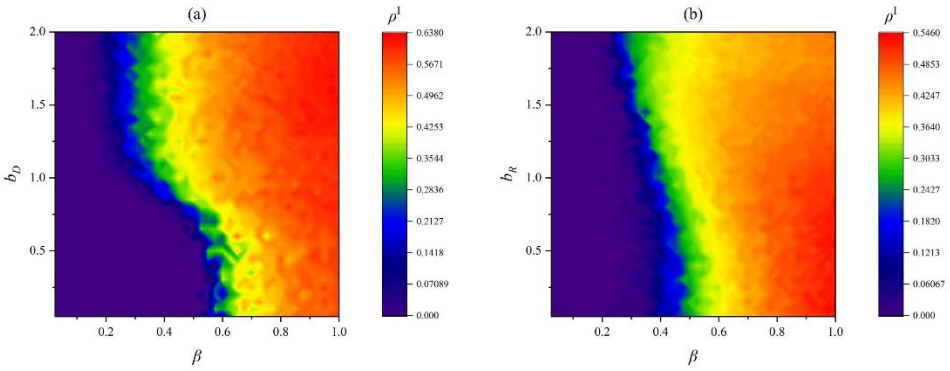


Figure 8. Effect of b_D and b_R on the model dynamics. (a) illustrates ρ^I as a function of β and the disconnection threshold b_D. Other paraments are set to $\omega = 0.8$, $a_R = b_R = 1$, and $\varphi = 0.8$. (b) illustrates ρ^I as a function of β and the reconnection threshold b_R. Other paraments are set to $\omega = 0.8$, $a_D = b_D = 1.3$, and $\varphi = 0.8$.

4.3. Effects of information adaptive thresholds on epidemic spreading

In this section, we investigate the effects of information adaptive reconnection threshold a_R and disconnection threshold a_D on the epidemic spreading dynamics. Figure 9(a)–(c) illustrated ρ^I as a function of epidemic spreading probability β and information transmission probability λ under different disconnection threshold a_D and reconnection threshold a_R. For Figure 9(a)–(c), the epidemic scale gradually decreases as the disconnection threshold a_D decreases. This occurs because a smaller disconnection threshold a_D causes more $U - A_2$ edges in the network to meet the disconnection threshold a_D and then disconnect, directly reducing channels for negative message transmission while allowing positive information to spread. Meanwhile, A_1 nodes have a lower probability of being infected, limiting the epidemic scale ρ^I and delaying the transmission threshold. Similarly, increasing the reconnection threshold a_R expands the epidemic scale ρ^I. This occurs because a higher reconnection threshold makes it more difficult to establish new $U - A_1$ connections, directly reducing positive message channels while allowing negative information to spread. Also, A_2 nodes can be easily infected, which leads to expanding the final epidemic scale ρ^I and advancing the transmission threshold. To further investigate the effects of information reconnection and disconnection thresholds on epidemic dynamics, Figure 10 depicts ρ^I as a function of infection probability β and the information reconnection threshold a_R and information disconnection threshold a_D.

As shown in Figure 10, similarly to the epidemic adaptive threshold, the information adaptive threshold also exhibits an inflection point. For Figure 10(a), when the disconnection threshold is small, most of the nodes satisfy the disconnection condition. Consequently, adaptive behavior occurs frequently. However, as the disconnection threshold a_D increases, fewer nodes meet the disconnection condition, making it easier for negative information to be transmitted within the network. This blocks the channels for positive information transmission, leading to a bigger final scale of epidemic spreading and advancing the epidemic spreading threshold. For Figure 10(b), when the information reconnection threshold is small, nearly all nodes satisfy the reconnection condition. However, as the information reconnection threshold a_R continues to increase, more nodes fail to meet the reconnection condition, staying in a negative information transmission environment. This promotes the transmission of negative information within the network, which leads to higher infection rates, thereby accelerating epidemic spreading and advancing the spreading threshold.

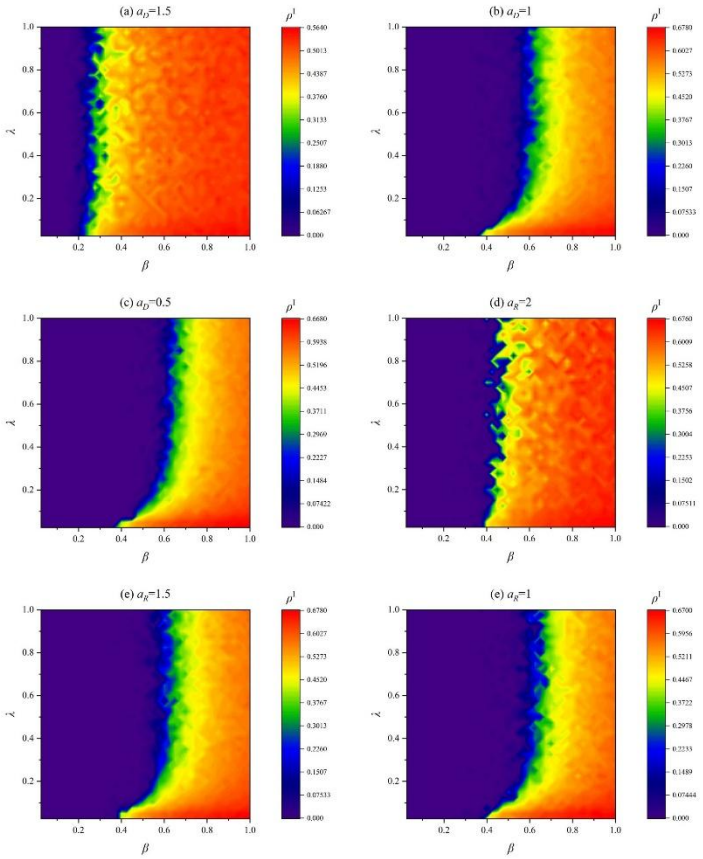


Figure 9. Illustrates ρ^I as a function of β and λ under different information disconnection and reconnection thresholds. The reconnection thresholds were set to (a) $a_D = 1.5$, (b) $a_D = 1$, and (c) $a_D = 0.5$. Other parameters were $\omega = 0.8$, $a_R = b_R = 1$, $b_D = 0.7$. The disconnection thresholds were set to (d) $a_R = 2$, (e) $a_R = 1.5$, and (f) $a_R = 1$. Other parameters were $\omega = 0.8$, $a_D = b_D = 0.7$, $b_R = 1$.

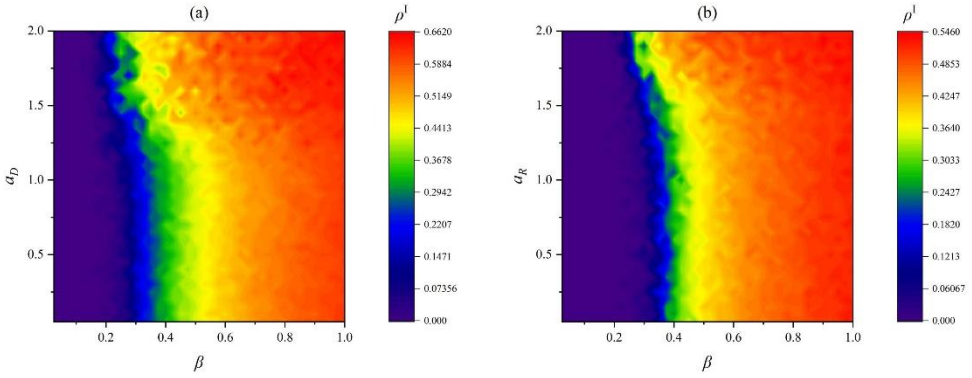


Figure 10. Effect of a_D and a_R on the model dynamics. (a) illustrates ρ^I as a function of β and the disconnection threshold a_D. Other paraments are set to $\omega = 0.8$, $a_R = b_R = 1$, $b_D = 1.3$, $\varphi = 0.8$. (b) illustrates ρ^I as a function of β and the reconnection threshold a_R. Other paraments are set to $\omega = 0.8$, $a_D = b_D = 1.3$, and $\varphi = 0.8$.

From the perspective of epidemic prevention, individuals with a positive and correct understanding of epidemics in real life can significantly lower their probability of being infected. Therefore, government and media should actively disseminate accurate information related to epidemics, educating people to promptly identify negative information and block connections with negative information, ensuring the majority of information channels are dominated by positive information. Similar to epidemic adaptive behavior, relevant authorities must also consider the cost. Once the vast majority of individuals possesses accurate information, costs can be reduced, minimizing unnecessary expenditure.

4.4. The impact of sensitivity on epidemic spreading

In this section, we investigate the impact of node sensitivity on epidemic spreading. Figure 11(a) shows the reconnection threshold of $a_R = b_R = 1$, and Figure 11(b) shows the disconnection threshold of $a_D = b_D = 1$. Higher sensitivity levels in both the information and epidemic layer suppress epidemic spreading and delay the epidemic spreading threshold. The value of a node's sensitivity directly determines the frequency of adaptive behavior within the network, and the frequency of adaptive behavior directly inhibits the spread of the epidemic. Therefore, a higher sensitivity level means a smaller scale of epidemic spreading. However, we can also observe that the effect of information sensitivity on suppressing epidemic spreading is smaller. This phenomenon offers practical implications for epidemic prevention in real life, as sensitivity levels partially reflect individuals' sensitivity to infection risks. Greater sensitivity enables faster responses to infected individuals, prompting timely self-protection strategies. Therefore, governments should strengthen public health education to promote widespread awareness of epidemic prevention.

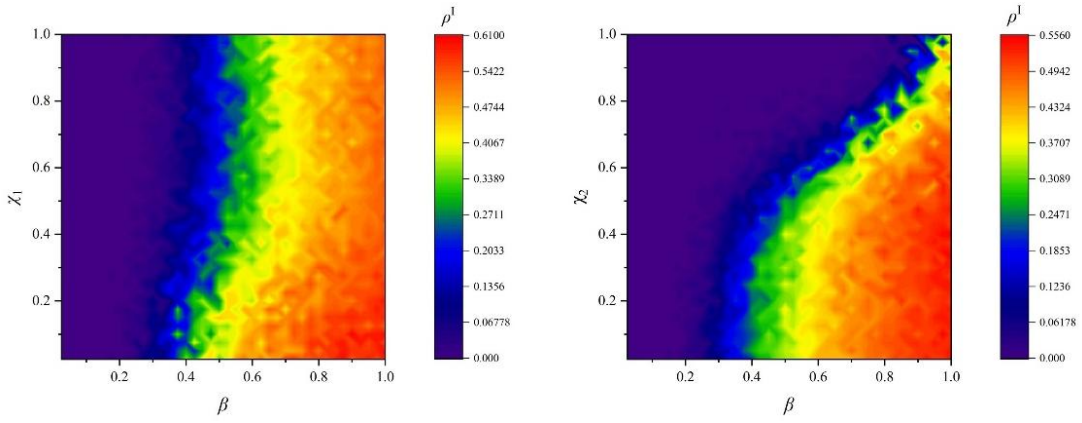


Figure 11. Effect of average information sensitivity χ_1 and average epidemic sensitivity χ_2 on model dynamics. Other parameters are $a_R = b_R = 1$, $a_D = b_D = 1$, $\omega = 0.8$, and $\varphi = 0.8$.

4.5. The impact of information-reducing factor on epidemic impact

Next, we investigate the impact of the information-reducing factor φ on the final scale of epidemic spread ρ^I. Figure 12 shows the effect of φ on the epidemic spreading scale ρ^I. We observe that as the information-reducing factor φ increases, the final scale of epidemic spread

expands, advancing the epidemic threshold. This occurs because, at the epidemic layer, φ directly affects the adaptive reconnection threshold b_R.

From a practical epidemic prevention perspective, the information-reducing factor can be interpreted as a priority of creating new edges. For an individual, knowing more epidemic-prevention information or measures may mean a lower probability of infection. Healthy individuals prefer to make connections with individuals with a lower infection risk. This not only indirectly increases the frequency of adaptive behavior but also means that newly created connections are safer. Therefore, relevant authorities should intensify public education on epidemic-related knowledge to ensure all individuals fully understand the epidemic, thereby reducing the scale of epidemic spreading.

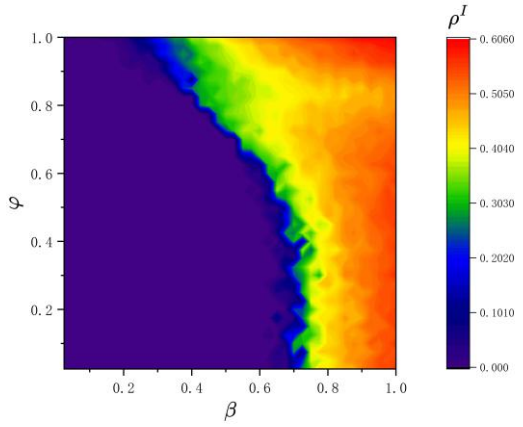


Figure 12. Effect of φ on the model dynamics. Other parameters are $a_R = b_R = 1$, $a_D = b_D = 0.7$, $\chi_1 = \chi_2 = 0.5$, and $\omega = 0.8$.

5. Conclusions

This study investigated the impact of adaptive thresholds on epidemic spreading in a two-layer adaptive network with asymmetric sensitivity. We defined the conditions governing adaptive disconnection and reconnection in the network using threshold functions. Specifically, a complete adaptive behavior occurs only when two thresholds are simultaneously satisfied, the sum of the sensitivity levels of two connected nodes exceeds the disconnection threshold, and the sum of the sensitivity levels of two unconnected nodes exceeds the reconnection threshold. We derived the propagation evolution equations for nodes and the epidemic spreading threshold using the MMCA method.

Monte Carlo simulation results further demonstrate that, within certain parameter ranges, both information adaptive thresholds and epidemic adaptive thresholds exert a significant influence on epidemic dynamics. In a certain range, decreasing the adaptive threshold effectively suppresses epidemic spreading and delays the outbreak threshold by increasing the frequency of adaptive behavior. Moreover, the adaptive threshold exhibits a non-monotonic, two-stage effect on the epidemic threshold. This is a qualitatively new phenomenon that arises from the individual's sensitivity heterogeneity and adaptive threshold mechanism, and it cannot be observed in models with no additional adaptive condition. If the value of the adaptive threshold is too big or too small, the effect of adaptive behavior will be smaller. In addition, the information-reducing factor can also suppress epidemic spreading by directly regulating the value of the reconnection threshold in the epidemic layer; a smaller reduction factor substantially decreases the epidemic scale and delays the transmission threshold, with a similar mechanism to the adaptive threshold. Node sensitivity levels also play a critical role in epidemic

spreading. In particular, under certain conditions, higher node sensitivity can suppress epidemic spreading and delay the spreading threshold by modulating the frequency of adaptive interactions.

For epidemic prevention, we suggest that improving public awareness of positive information is a prerequisite for unaware and susceptible individuals to effectively adopt adaptive preventive behaviors. Although unaware nodes can distinguish positive and negative information to a certain measure, only when they have the ability to accurately acquire correct epidemic-related information can they adopt adaptive behavior in a timely manner. However, the ability to distinguish different categories of information is not acquired by every individual in real life. Additionally, the government and media should actively disseminate positive information about the epidemic, minimizing the emergence of misinformed individuals who spread negative information in the network. Moreover, raising the sensitivity level of individuals to risk and infection lowers their tolerance to the epidemic. As an epidemic is discovered nearby, adaptive behavior is timely adopted, reducing the time of direct exposure to the epidemic. Our research contributes novel insights into adaptive behaviors at both the information and epidemic levels.

While we have made progress in exploring additional conditions of adaptive behavior, several areas still need deeper investigation. For instance, our simulations were conducted on artificially generated networks, but real-world networks are often more complex. Furthermore, in adaptive behavior, although connections with infected individuals were broken at the current time step, newly connected susceptible individuals remain vulnerable to infection in the next time steps. Moreover, epidemic spreading displays a probability of indirect spreading in real life, which suggests that, after breaking the connection between infected individuals, susceptible individuals may still be at risk of being infected by indirect spreading. Therefore, in our subsequent work, we will extend this model to indirect spreading.

Use of AI tools declaration

The authors declare they have not used artificial intelligence (AI) tools in the creation of this article.

Acknowledgements

This work was partially supported by the Project for the National Natural Science Foundation of China (72574145, 72174121), the Project for the National Social Science Foundation of China (24BGL281), and the Program for Professor of Special Appointment (Eastern Scholar) at Shanghai Institutions of Higher Learning, and the Project for Oriental Talent Program of Shanghai.

Conflict of interest

All authors declare no conflicts of interest in this paper.

Author contributions

Liang'an Huo: Conceptualization, Funding acquisition, Investigation, Methodology, Project administration, Resources, Supervision, Writing-review & editing.

Xingyu Wan: Data curation, Formal analysis, Investigation, Methodology, Visualization, Writing-original draft.

Xu Xu: Formal analysis, Writing-review & editing.
Minghua Liu: Formal analysis, Writing-review & editing.

References

1. A. M. Alotaibi, Explainable long-sequence time-series forecasting for infectious diseases using optimised transformer models, *Int. J. Data Sci. Anal.*, **21** (2026), 8. https://doi.org/10.1007/s41060-025-00930-9
2. J. Wang, X. Yan, X. Chang, Dynamics analysis and optimal control of SIR-w infectious disease model under the influence of multidimensional information, *J. Math. Anal. Appl.*, **553** (2026), 129855. https://doi.org/10.1016/j.jmaa.2025.129855
3. C. Zheng, C. Xia, Q. Guo, M. Dehmer, Interplay between SIR-based disease spreading and awareness diffusion on multiplex networks, *J. Parallel Distrib. Comput.*, **115** (2018), 20–28. https://doi.org/10.1016/j.jpdc.2018.01.001
4. H. Wang, H. Huang, H. Liu, Competition or cooperation? Multiple information diffusion against epidemic spreading in a multiplex network, *Chaos Solitons Fractals*, **203** (2026), 117585. https://doi.org/10.1016/j.chaos.2025.117585
5. Y. Liu, M. Tang, Y. Zhou, The impact of high-order multi-source information verification mechanisms on propagation dynamics in multilayer high-order networks, *Chaos Solitons Fractals*, **203** (2026), 117715. https://doi.org/10.1016/j.chaos.2025.117715
6. Q. Yin, Z. Wang, K. Wang, Z. Hong, Coupled dynamics of information-epidemic spreading with resource allocation and transmission on multi-layer networks, *Entropy*, **27** (2025), 1080. https://doi.org/10.3390/e27101080
7. W. O. Kermack, A. G. McKendrick, A contribution to the mathematical theory of epidemics, *Proc. R. Soc. A*, **115** (1927), 700–721. https://doi.org/10.1098/rspa.1927.0118
8. T. Su, Y. Kao, D. Jiang, Dynamical behaviors of a stochastic SIR epidemic model with reaction-diffusion and spatially heterogeneous transmission rate, *Chaos Solitons Fractals*, **195** (2025), 116283. https://doi.org/10.1016/j.chaos.2025.116283
9. H. Bao, Y. He, Epidemic dynamics with awareness cascade of positive and negative information on delayed multiplex networks, *Chaos*, **35** (2025), 023135. https://doi.org/10.1063/5.0247513
10. H. Shi, Z. Duan, G. Chen, An SIS model with infective medium on complex networks, *Phys. A*, **387** (2008), 2133–2144. https://doi.org/10.1016/j.physa.2007.11.048
11. D. Han, X. Wang, Impact of positive and negative information on epidemic spread in a three-layer network, *Chaos Solitons Fractals*, **186** (2024), 115264. https://doi.org/10.1016/j.chaos.2024.115264
12. Y. Zhang, X. Gou, W. Zhou, J. Ma, The role of information dissemination in suppressing epidemic spreading in multiplex networks, *Phys. Lett. A*, **560** (2025), 130950. https://doi.org/10.1016/j.physleta.2025.130950
13. M. Nekovee, Y. Moreno, G. Bianconi, M. Marsili, Theory of rumour spreading in complex social networks, *Phys. A*, **374** (2007), 457–470. https://doi.org/10.1016/j.physa.2006.07.017
14. Z. Huang, X. Shu, Q. Xuan, Z. Ruan, Epidemic spreading under game-based self-quarantine behaviors: The different effects of local and global information, *Chaos*, **34** (2024), 013112. https://doi.org/10.1063/5.0180484

15. H. Bao, X. Wu, Epidemic propagation with competitive information in multiplex networks with simplicial complexes, *Chaos Solitons Fractals*, **201** (2025), 117254. https://doi.org/10.1016/j.chaos.2025.117254
16. J. Ma, P. Wang, Impact of community networks with higher-order interaction on epidemic dynamics, *Chaos Solitons Fractals*, **180** (2024), 114471. https://doi.org/10.1016/j.chaos.2024.114471
17. S. Funk, E. Gilad, C. Watkins, V. A. A. Jansen, The spread of awareness and its impact on epidemic outbreaks, *Proc. Natl. Acad. Sci. U.S.A.*, **106** (2009), 6872–6877. https://doi.org/10.1073/pnas.0810762106
18. C. Granell, S. Gómez, A. Arenas, Dynamical interplay between awareness and epidemic spreading in multiplex networks, *Phys. Rev. Lett.*, **111** (2013), 128701. https://doi.org/10.1103/PhysRevLett.111.128701
19. C. Granell, S. Gómez, A. Arenas, Competing spreading processes on multiplex networks: Awareness and epidemics, *Phys. Rev. E*, **90** (2014), 012808. https://doi.org/10.1103/PhysRevE.90.012808
20. Z. Zhang, K. Zhu, F. Wang, Indirect information propagation model with time-delay effect on multiplex networks, *Chaos Solitons Fractals*, **192** (2025), 115936. https://doi.org/10.1016/j.chaos.2024.115936
21. L. Liu, S. Geng, L. Wei, Z. Lu, Y. Ma, Dynamics of two-strain disease transmission with negative vaccine information and vaccination on multiplex networks, *Appl. Math. Comput.*, **510** (2026), 129701. https://doi.org/10.1016/j.amc.2025.129701
22. J. Song, W. Li, Y. Xiao, L. Chen, C. Yang, L. Qi, et al., Optimal information spreading strategy for containing epidemic spreading on higher order multiplex networks, *Appl. Math. Comput.*, **511** (2026), 129725. https://doi.org/10.1016/j.amc.2025.129725
23. D. Yang, W. Zhang, Z. Li, Z. Lin, N. Meng, J. Xian, et al., Coupled awareness-epidemic spreading incorporating the impact of self-media, *Chaos Solitons Fractals*, **205** (2026), 117824. https://doi.org/10.1016/j.chaos.2025.117824
24. X. Sun, L. Zhang, P. Zheng, Coevolution of information and epidemics in multiplex networks under risk-perception and higher-order interactions, *Appl. Math. Comput.*, **522** (2026), 129936. https://doi.org/10.1016/j.amc.2025.129936
25. L. Y. Liu, C. R. Cai, S. P. Zhang, B. Q. Li, Coexistence of positive and negative information in information-epidemic dynamics on multiplex networks, *Phys. A*, **666** (2025), 130534. https://doi.org/10.1016/j.physa.2025.130534
26. D. Guo, S. Trajanovski, R. van de Bovenkamp, H. Wang, P. Van Mieghem, Epidemic threshold and topological structure of susceptible-infectious-susceptible epidemics in adaptive networks, *Phys. Rev. E*, **88** (2013), 042802. https://doi.org/10.1103/PhysRevE.88.042802
27. Y. R. Song, G. P. Jiang, Y. W. Gong, Epidemic propagation on adaptive coevolutionary networks with preferential local-world reconnecting strategy, *Chin. Phys. B*, **22** (2013), 040205. https://doi.org/10.1088/1674-1056/22/4/040205
28. P. Zhu, Q. Zhi, Y. Guo, Z. Wang, Analysis of epidemic spreading process in adaptive networks, *IEEE Trans. Circuits Syst. II Express Briefs*, **66** (2019), 1252–1256. https://doi.org/10.1109/TCSII.2018.2877406

29. M. Mancastroppa, R. Burioni, V. Colizza, A. Vezzani, Active and inactive quarantine in epidemic spreading on adaptive activity-driven networks, *Phys. Rev. E*, **102** (2020), 020301. https://doi.org/10.1103/PhysRevE.102.020301
30. X. Hong, G. Zhang, Z. Tian, B. Wang, D. Lu, Integrating adaptive rewiring and compulsory regulating: Co-evolutionary epidemic dynamics driven by multi-source information, *IEEE Trans. Networks Sci. Eng.*, **13** (2026), 6622–6639. https://doi.org/10.1109/TNSE.2026.3657856
31. X. L. Peng, Y. D. Zhang, Contagion dynamics on adaptive multiplex networks with awareness-dependent rewiring, *Chin. Phys. B*, **30** (2021), 058901. https://doi.org/10.1088/1674-1056/abe1ab
32. Y. Guo, L. Tu, X. Wang, The coupled dynamics of awareness and disease: Based on the adaptive mechanism and the surroundings reinforcement, *Phys. A*, **649** (2024), 129949. https://doi.org/10.1016/j.physa.2024.129949
33. W. Xiong, C. Zhou, Epidemic spreading with an awareness-based adaptive mechanism in temporal multiplex networks, *Front. Phys.*, **11** (2023), 1285480. https://doi.org/10.3389/fphy.2023.1285480
34. M. Li, L. Huo, Y. Dong, X. Xie, Y. Cheng, Effect of individual heterogeneity on the coupled spread of information and disease in higher-order multiplex networks, *Nonlinear Dyn.*, **113** (2025), 10659–10679. https://doi.org/10.1007/s11071-024-10633-8
35. Y. Qian, D. Zhao, C. Xia, M. Perc, Information flow in psychological evolutionary decision-making on multiplex networks: A survey and beyond, *IEEE Trans. Networks Sci. Eng.*, **13** (2026), 1128–1146. https://doi.org/10.1109/TNSE.2025.3591446
36. Y. Pan, Z. Yan, The impact of individual heterogeneity on the coupled awareness-epidemic dynamics in multiplex networks, *Chaos*, **28** (2018), 063123. https://doi.org/10.1063/1.5000280
37. C. Liu, L. X. Zhou, C. J. Fan, L. A. Huo, Z. W. Tian, Activity of nodes reshapes the critical threshold of spreading dynamics in complex networks, *Phys. A*, **432** (2015), 269–278. https://doi.org/10.1016/j.physa.2015.03.054
38. X. Zhang, H. Deng, Z. Ruan, X. Zhang, Coevolution of epidemic spread and protective behavior in populations with heterogeneous behavioral tendencies, *Phys. A*, **687** (2026), 131376. https://doi.org/10.1016/j.physa.2026.131376.
39. J. Shi, L. Zhu, Epidemic spreading on heterogeneous probabilistic activity driven network model, *Nonlinear Dyn.*, **114** (2026), 161. https://doi.org/10.1007/s11071-025-12206-9
40. M. Li, L. Huo, Effect of time-varying validity of individual interaction on co-evolution of awareness and epidemics in a multiplex high-order network, *Appl. Math. Comput.*, **499** (2025), 129396. https://doi.org/10.1016/j.amc.2025.129396
41. M. Gao, L. Zhu, S. Shen, Epidemic propagation dynamic on the higher-order multilayer network, *Chaos Solitons Fractals*, **200** (2025), 116922. https://doi.org/10.1016/j.chaos.2025.116922
42. M. Wang, L. Peng, B. Jia, L. Hong, Epidemic dynamics in physical-information-social multilayer networks, *Phys. A*, **678** (2025), 130944. https://doi.org/10.1016/j.physa.2025.130944
43. Z. Zhang, K. Zhu, F. Wang, L. Liu, L. Wang, Effects of isolation and information dissemination on epidemic dynamics in multiplex networks, *Chaos Solitons Fractals*, **199** (2025), 116889. https://doi.org/10.1016/j.chaos.2025.116889
44. S. Mongolian, Y. Kao, C. Wang, H. Xia, Robust mean square stability of delayed stochastic generalized uncertain impulsive reaction-diffusion neural networks, *J. Frankl. Inst.*, **358** (2021), 877–894. https://doi.org/10.1016/j.jfranklin.2020.04.011

45. F. Zhang, M. Hua, F. Deng, J. Fei, H. Chen, Quantized output feedback tracking control for discrete-time periodic Markov jump systems with packet loss compensation, *IEEE Trans. Autom. Sci. Eng.*, **22** (2025), 8480–8491. https://doi.org/10.1109/TASE.2024.3486067



AIMS Press

©2026 the Author(s), licensee AIMS Press. This is an open access article distributed under the terms of the Creative Commons Attribution License (https://creativecommons.org/licenses/by/4.0)